White Rose Research Online

eprints@whiterose.ac.uk
https://eprints.whiterose.ac.uk
Universities of Leeds, Sheffield and York

Deposited via The University of Leeds.

White Rose Research Online URL for this paper:
https://eprints.whiterose.ac.uk/id/eprint/83575/

Version: Accepted Version

Article:
Mullis, AM, Rosam, J and Jimack, PK (2010) Solute trapping and the effects of anti-trapping currents on phase-field models of coupled thermo-solutal solidification. Journal of Crystal Growth, 312 (11). 1891 - 1897. ISSN: 0022-0248

https://doi.org/10.1016/j.jcrysgro.2010.03.009

Reuse
Items deposited in White Rose Research Online are protected by copyright, with all rights reserved unless indicated otherwise. They may be downloaded and/or printed for private study, or other acts as permitted by national copyright laws. The publisher or other rights holders may allow further reproduction and re-use of the full text version. This is indicated by the licence information on the White Rose Research Online record for the item.

Takedown
If you consider content in White Rose Research Online to be in breach of UK law, please notify us by emailing eprints@whiterose.ac.uk including the URL of the record and the reason for the withdrawal request.

UNIVERSITY OF LEEDS
University of Sheffield
UNIVERSITY of York

Solute Trapping and the Effects of Anti-Trapping Currents on Phase-Field Models of Coupled Thermo-Solutal Solidification

A.M. Mullis[*§], *J. Rosam*[§‡] *& P.K. Jimack*[‡]

Institute for Materials Research[§] and School of Computing[‡],

University of Leeds, Leeds LS2 9JT, UK.

Key Words: Solidification: rapid solidification, Phase-field modelling,

Abstract

We explore how the inclusion of an anti-trapping current within a phase-field model of coupled thermo-solutal growth formulated in the thin interface limit actually affects the observed levels of solute trapping during dendritic growth. The problem is made computational tractable by the use of advanced numerical techniques including local mesh adaptivity, implicit temporal discreteization and a multigrid solver. Contrary to published results for pure solutal models we find that the inclusion of such an anti-trapping current does not lead to the recovery of the equilibrium partition coefficient, except in the limit of very slow growth. At higher growth velocities non-vanishing amounts of solute trapping are observed.

* Corresponding Author, e-mail : A.M.Mullis@leeds.ac.uk

tel : +44-113-343-2568

fax : +44-113-343-2384

Introduction

Dendritic growth has been a subject of enduring scientific interest, both because it is a prime example of spontaneous pattern formation and due to the propensity of many metals to solidify dendritically from their parent melt. Moreover, remnants of these dendritic microstructures often survive subsequent processing operations, such as rolling and forging and thereafter have a pervasive influence on the engineering properties of these metals.

In recent years significant progress towards understanding dendritic growth has been afforded by phase-field modelling. However, the application of phase-field modelling has largely been restricted to two limiting cases; namely the thermally controlled growth of pure substances [e.g. 1, 2]and the solidification of relatively concentrated alloys and solutions [e.g. 3, 4], wherein growth is sufficiently slow that the problem may be considered isothermal. However, in the cases of the solidification of very dilute alloys and of rapid solidification processing the isothermal approximation is no longer valid and it becomes necessary to solve the problem for coupled heat and solute transport.

Two basic formulations of the coupled phase-field problem have been reported in the literature. The first, which is due to Loginova *et al*.[5], follows on from the derivation of the solutal model of Warren & Boettinger[6]. However, there are doubts about the quantitative validity of this model[7] as the numerical results display excess solute trapping and have an unresolved interface width dependence. This methodology has been extended numerically by Lan *et al*.[8], who introduced an adaptive finite volume solver, which allowed them to use realistic values of *Le*, although this did not overcome either the excess solute trapping or the interface-width dependence observed in the solution. An alternative formulation of the coupled phase-field problem based on the Karma thin interface model[9] has been presented by Ramirez & Beckermann[10, 7] and has been extended numerically by ourselves[11, 12] to incorporate a fully adaptive, fully implicit, multigrid solver, allowing higher Lewis numbers and lower undercoolings to be studied. As the thin interface model has been shown to be independent of the length scale chosen for the mesoscopic diffuse interface width, it is capable of giving quantitatively correct predictions for dendritic growth velocity, *V*, and tip

radius, ρ. Moreover, the inclusion of an anti-trapping current[9] within this formulation of the coupled problem should ensure that the problems associated with excess solute trapping observed in the models of [5, 8] are overcome.

For the growth of a dendrite under solute only control it was shown in [9] that the inclusion of an anti-trapping current effectively totally suppresses solute trapping. However, the growth velocities observed for solutal dendrites may be very low compared to that for dendrites growing under coupled thermo-solutal control, and consequently it is not clear what effect the inclusion of an anti-trapping current within a coupled thermo-solutal model of dendritic growth will have. That is the subject of this paper.

During equilibrium solidification solute will partition between the solid and the liquid such that the concentrations, c_s^0 and c_l^0, at the interface location in the solid and liquid phases respectively are in a fixed ratio,

$$k_E = \frac{c_s^0}{c_l^0} \tag{1}$$

where k_E is the equilibrium partition coefficient and can be obtained from the location of the liquidus and solidus lines on the phase diagram. This partitioning of solute ensures that the chemical potentials on either side of the interface remain equal. However, as we depart from equilibrium by increasing the growth velocity, V, either by undercooling the melt or by imposing large thermal gradients to effect rapid heat extraction, the actual ratio c_s^0 / c_l^0 moves away from k_E and begins to approach 1. This process of solute trapping has been shown by Aziz[13, 14] to give rise to a velocity-dependant partition coefficient, $k(V)$, which follows the relationship

$$k(V) = \frac{k_E + \beta}{1 + \beta} \tag{2}$$

where β is a dimesionless growth velocity which is generally written as either $\beta = V/V_D$, where V_D is a characteristic diffusive velocity for atoms at the solid-liquid interface, or as $\beta = V\lambda/D_i$, where λ_i is a measure of the solid-liquid interface width and D_i is an interface diffusion coefficient. In this latter case β takes the form of an interface Peclet number.

Description of the Model

The starting point for our investigation into the extent of solute trapping within coupled thermo-solutal phase-field models of solidification is the definition of a free energy functional,

$$\mathscr{F} = \int_V f(\phi, c, T) + \frac{\sigma_c}{2}|\nabla c|^2 + \frac{\sigma_\phi}{2}|\nabla \phi|^2 \, dV \tag{3}$$

where $\phi(\mathbf{x}, t)$ is the phase variable, which takes values +1 in the solid phase and -1 in the liquid phase, $c(\mathbf{x}, t)$ is the local concentration of component B in A and T is the absolute temperature. σ_c and σ_ϕ are the gradient entropy coefficients which ensure the increase in entropy throughout solidification, although here, as in most other phase-field simulations, we assume $\sigma_c = 0$, while σ_ϕ is related to the width of the diffuse interface, W, via the relation $\sigma_\phi = W^2 H$. $f(\phi, c, T)$ is the local free energy which may be written,

$$f(\phi, c, T) = \tilde{f}(\phi, T_M) + f_{AB}(\phi, c, T) \tag{4}$$

where the first term on the right-hand side is the sum of the free energies of the pure materials with melting temperature T_M, and has the standard form of a double-well potential with barrier height H,

$$\tilde{f}(\phi, T_M) = H\left(\frac{\phi^4}{4} - \frac{\phi^2}{2}\right) \tag{5}$$

while the second term is the free energy due to the solute addition. The form of $f_{AB}(\phi, c, T)$ has been derived in [10] and [15] on the basis of the equilibrium properties that follow from the two conditions

$$\frac{\delta \mathscr{F}}{\delta c} = \mu_E \quad \text{and} \quad \frac{\delta \mathscr{F}}{\delta \phi} = 0 \tag{6}$$

where μ_E is the spatially uniform value of the chemical potential. The first condition is used to determine the form of the equilibrium partition coefficient, k_E, and the equilibrium concentration profile while the second leads to the form of $f_{AB}(\phi, c, T)$, which is given as,

$$f_{AB}(\phi, c, T) = \frac{RT_M}{v_0 m} \exp\left\{\frac{\ln k_E}{2}(1 + \tilde{g}(\phi))\right\}\Delta T + \frac{RT_M}{v_0}(c \ln c - c) + c(\bar{\varepsilon} + \tfrac{1}{2}\tilde{g}(\phi)\Delta\varepsilon) \tag{7}$$

where R is the universal gas constant, v_0 is the molar volume (which we assume constant), m is the slope of the liquidus line, $\Delta T = T_M - T$ is the undercooling. $\tilde{g}(\phi)$ is an interpolating function that satisfies the conditions $\tilde{g}(\pm 1) = \pm 1$ and $\tilde{g}'(\pm 1) = 0$, and

$$\bar{\varepsilon} = \frac{\tilde{\varepsilon}_s + \tilde{\varepsilon}_l}{2} \quad , \quad \Delta\varepsilon = \tilde{\varepsilon}_s - \tilde{\varepsilon}_l \tag{8}$$

where $\tilde{\varepsilon}_s$ and $\tilde{\varepsilon}_l$ are the free energy densities of the pure solid and pure liquid phases respectively.

The evolution of the phase and concentration fields are given by

$$\frac{\partial \phi}{\partial t} = -K_\phi(T)\frac{\delta \mathscr{F}}{\delta \phi} \tag{9}$$

and

$$\frac{\partial c}{\partial t} = \nabla \cdot \left(K_c \nabla \frac{\delta \mathscr{F}}{\partial c} - j_{at} \right) \tag{10}$$

where K_ϕ is the atomic mobility at the interface and

$$K_c = \frac{v_0}{RT_M} Dq(\phi) \tag{11}$$

where D is the diffusivity of the solute in the liquid phase and $q(\phi)$ is an interpolating polynomial that describes how the diffusivity varies across the solid-liquid interface. For an asymmetric system, which is appropriate to solute transport (i.e. the diffusivity in the solid is very much smaller than that in the liquid), we require $q(1) = 1$ and $q(-1) = 0$.

Here the first term inside the bracket in Eq. (10) is a manifestation of Fick's law for diffusion in the liquid while the second term is an anti-trapping current as first proposed by [9], which takes the form,

$$j_{at} = -ac_\infty (1 - k_E) We^u \frac{\partial \phi}{\partial t} \frac{\nabla \phi}{|\nabla \phi|} \tag{12}$$

where c_∞ is the far-field solute concentration, a is an adjustable parameter which controls the magnitude of the anti-trapping current, the value of which will be discussed later and u is a dimensionless variable given by

$$u = \ln\left(\frac{c}{c_\infty}\right) - \tfrac{1}{2} \ln k_E [\tilde{g}(\phi) + 1] \rightarrow \ln\left(\frac{c}{c_\infty}\right) - \tfrac{1}{2} \ln k_E [h(\phi) + 1] \tag{13}$$

Here the interpolating function $\tilde{g}(\phi)$ may be replaced by the function $h(\phi)$. This is permitted as $\tilde{g}(\phi)$ enters into the equations for the evolution of both the phase and concentration fields, but the actual requirements on the interpolating function are less stringent in the concentration equation than in the phase equation[15]. Specifically, while it is still required that $h(\pm 1) = \pm 1$, we do not require $h'(\pm 1) = 0$, which subsequently allows the simpler choice $h(\phi) = \phi$ to be made.

The purpose of the anti-trapping current is to provide a solute flux normal to the diffuse interface from the solid into the liquid thus counterbalancing the tendency of phase-field models to display unphysically high levels of solute trapping. This tendency for solute trapping is an inherent property of diffuse interface models that do not include an anti-trapping current and gives rise to a level of solute trapping that is dependant upon the width chosen for the diffuse interface. As the interface width is generally set considerably larger than could be considered physical, excess amounts of solute trapping result.

Evaluating the variational derivative (8) and applying the non-dimensionalisations

$$U = \frac{e^u - 1}{1 - k_E} \quad \text{and} \quad \theta = \frac{\Delta T - mc_\infty}{L / c_p} \tag{14}$$

where m is the slope of the liquidus line, L is the latent heat on fusion and c_p is the specific heat, the phase and concentration equations may be obtained as[10]

$$\tau \frac{\partial \phi}{\partial t} = W^2 \nabla^2 \phi - f'(\phi) - \lambda g'(\phi)(\theta + Mc_\infty U) \tag{15}$$

and

$$\frac{1 + k_E}{2} \frac{\partial U}{\partial t} = \nabla \cdot \left(Dq(\phi) \nabla U + aW[1 + (1 - k_E)U] \frac{\partial \phi}{\partial t} \frac{\nabla \phi}{|\nabla \phi|} \right) + \frac{1}{2} \frac{\partial}{\partial t} \{h(\phi)[1 + (1 - k_E)U]\} \tag{16}$$

where M is the scaled slope of the liquidus line,

$$M = -\frac{m(1 - k_E)}{L / c_p} \tag{17}$$

λ is a coupling parameter,

$$\lambda = -\frac{15}{8}\frac{RT_M(1-k_E)L}{2\nu_0 H c_p m} \tag{18}$$

τ is a characteristic time for attachment at the interface,

$$\tau = \frac{1}{K_\phi(T)H} \tag{19}$$

and $g(\phi) = 8\tilde{g}(\phi)/15$.

Finally, the temperature equation is just the standard thermal diffusion equation with a source term, namely

$$\frac{\partial\theta}{\partial t} = \alpha\nabla^2\theta + \frac{1}{2}\frac{\partial\phi}{\partial t} \tag{20}$$

In order to formulate the phase-field model in such a way that the results do not depend upon the width, W, of the diffuse interface the thin-interface analysis is applied, in which the system is transformed onto a local orthogonal curvilinear co-ordinate system (ξ_1, ξ_2, ξ_3) which co-moves with the interface and in which ξ_3 measures signed distance from the level line $\phi = 0$. Asymptotic expansions of the solution,

$$\begin{aligned}\phi &= \phi_0 + p\phi_1 + p^2\phi_2 + \ldots \\ U &= U_0 + pU_1 + p^2U_2 + \ldots \\ \theta &= \theta_0 + p\theta_1 + p^2\theta_2 + \ldots\end{aligned} \tag{21}$$

on the inner and outer regions of the solid-liquid interface are matched to obtain an equation set in which the solution is independent of the width of the diffuse interface. Here, p is a Peclet number given by $p = WV/D$, where V is the local growth velocity,

$$\phi_0 = -\tanh\left(\frac{\eta}{\sqrt{2}}\right) \tag{22}$$

where $\eta = \xi_3/p$ and we use the convention

$$\theta_k = \frac{1}{k!}\frac{\partial^k \theta}{\partial p^k}\bigg|_{p=0} \tag{23}$$

which is also applied to both U and ϕ.

Physically, this analysis corrects for the effects of lateral concentration gradients along the interface, interface stretching (the fact that when curved a diffuse interface is longer on one side than the other) and the excess solute trapping described above.

The analysis has previously been presented for a coupled model by [10], wherein results identical to that for the solute only case studied in [9] were recovered. For this reason we do not here repeat the analysis, only drawing attention to some points that we consider salient to a discussion of solute-trapping phenomena within the coupled phase-field model. Specifically, we note that the first order (in p) solutions for U and θ are,

$$U_1 = \overline{U}_1 + \tfrac{1}{2}\left[1 + (1-k_E)U_0\right]\int_0^\eta p\left(\phi_0(\eta')\right)d\eta' \tag{24}$$

$$\theta_1 = \overline{\theta}_1 + A_\theta \eta + \frac{1}{2Le}\int_0^\eta \phi_0(\eta')\,d\eta' \tag{25}$$

where $p(\phi_0)$ is the function

$$p(\phi_0) = \frac{h(\phi_0) - 2a\frac{\partial \phi_0}{\partial \eta} - 1}{q(\phi_0)} \tag{26}$$

and Eq. (24) is the same as that obtained for the thin interface analysis of the isothermal solute problem[9]. If we now adopt $h(\phi) = \phi$, this being the simplest function that satisfies the restrictions on h above, and $a = 1/(2\sqrt{2})$ which has been shown in the isothermal case to eliminate the jump in chemical potentials on either side of the interface[15, 9], with $q(\phi) = ½(1-\phi)$ as defined above we have $p(\phi_0) = (\phi_0 - 1)$. That is, the form of the integral in Eq. (24) reduces to the same form as that in Eq. (25), which is the also the same form as in the thin interface analysis of the pure thermal problem.

In the isothermal model other values of a are permitted should non-zero amounts of solute trapping be desired, a point specifically comment upon by [9], although this does require a re-evaluation of the integral

$$K = \int_{-\infty}^{+\infty} g'(\phi_0) \frac{\partial \phi_0}{\partial \eta} \left[\int_0^{\eta} p(\phi_0(\eta')) d\eta' \right] d\eta \tag{27}$$

However, in the coupled model the situation is more restrictive in that we require U_i and θ_i to have the same form in order for the analysis to be tractable, a point that is perhaps not clear in the derivation of the coupled model presented in [10], as the substitution $h(\phi) = \phi$ and $a = 1/(2\sqrt{2})$ have already been made when the integrals for U_1 and θ_1 are formulated. However, the implication of this is that once the choice $h(\phi) = \phi$ has been made, the thin interface analysis for the coupled thermo-solutal model can only be performed for $a = 1/(2\sqrt{2})$ and that this is therefore the only value for which the model is valid. Understanding how the anti-trapping current with $a = 1/(2\sqrt{2})$ effects the solute trapping behaviour of the coupled model is therefore an important issue.

Following the thin-interface analysis given in [10] we arrive at the equations governing the evolution of the coupled concentration, thermal and anisotropic phase fields, non-dimensionalised against the characteristic length and time scales W_0 and τ_0 respectively as,

$$A^2(\psi)\left[\frac{1}{Le}+Mc_\infty\left[1+(1-k_E)U\right]\right]\frac{\partial\phi}{\partial t}=\nabla\cdot\left(A^2(\psi)\nabla\phi\right)+\phi(1-\phi^2)$$
$$-\lambda(1-\phi^2)^2(\theta+Mc_\infty U)-\frac{\partial}{\partial x}\left(A(\psi)A'(\psi)\frac{\partial\phi}{\partial y}\right)+\frac{\partial}{\partial y}\left(A(\psi)A'(\psi)\frac{\partial\phi}{\partial x}\right) \tag{28}$$

$$\left(\frac{1+k_E}{2}-\frac{1-k_E}{2}\phi\right)\frac{\partial U}{\partial t}=\nabla\cdot\left(D\frac{1-\phi}{2}\nabla U+a\left|1+(1-k_E)U\right|\frac{\partial\phi}{\partial t}\frac{\nabla\phi}{|\nabla\phi|}\right)$$
$$+\frac{1}{2}\left(\left|1+(1-k_E)U\right|\frac{\partial\phi}{\partial t}\right) \tag{29}$$

$$\frac{\partial\theta}{\partial t}=\alpha\nabla^2\theta+\frac{1}{2}\frac{\partial\phi}{\partial t} \tag{30}$$

where $\psi=\arctan(\phi_x/\phi_y)$ is the angle between the normal to the interface and the *x*-axis and $A(\psi) = 1 + \varepsilon.\cos(\eta\psi)$ is an anisotropy function with strength ε and mode number η. The characteristic length and time scales are given by

$$W_0=\frac{d_0D}{a_1a_2}\ ,\qquad \tau_0=\frac{d_0^2a_2\lambda^3}{Da_1^2} \tag{31}$$

The dimensionless coupling parameter, λ, results from the thin interface analysis and is given as[10, 9],

$$\lambda=\frac{D}{a_2}=\frac{a_1W_0}{d_0} \tag{32}$$

where d_0 is the chemical capillary length and the constants a_1 and a_2 are given by

$$a_1=\frac{I}{J}=\frac{5\sqrt{2}}{8}\ ,\qquad a_2=\frac{K+FJ}{2J}=0.6267 \tag{33}$$

with K as given in Eq. (27) and

$$I = \int_{-\infty}^{+\infty} \left[\frac{\partial \phi_0}{\partial \eta} \right]^2 d\eta \tag{34}$$

$$J = \int_{-\infty}^{+\infty} g'(\phi_0) \frac{\partial \phi_0}{\partial \eta} \partial \eta \tag{35}$$

$$F = \int_{0}^{+\infty} (\phi_0 + 1) d\eta \tag{36}$$

Numerical Methods

The governing equations are descritized using a finite difference approximation based upon a quadrilateral, non-uniform, locally-refined mesh with equal grid spacing in both directions. This allows the application of standard second order central difference stencils for the calculation of first and second differentials, while a compact 9-point scheme has been used for Laplacian terms, in order to reduce the mesh induced[16] anisotropy. The mesh data is stored in a quadtree data structure as in [17, 18].

In order to ensure that sufficient levels of refinement occur around the interface region and that the extreme multi-scale nature of the thermal and solutal diffusion fields at high Lewis numbers are handled appropriately, adaptive refinement is based upon an elementwise gradient criterion given by

$$E = h_{|\nu|} \left(|\nabla \phi| + E_C |\nabla U| + E_T |\nabla \theta| \right) \tag{37}$$

where $h_{|\nu|}$ is the element size on the finest level of refinement and E_C and E_T are user-defined constants which control the respective effect of the concentration and thermal fields relative to the phase-field. These are compared to two tolerances, E_{Tol}^{+} and E_{Tol}^{-}. If, at any location within the domain $E \geq E_{Tol}^{+}$ the mesh is refined at that location while conversely if $E \leq E_{Tol}^{-}$ the mesh is permitted to coarsen at that location (subject to geometric constraints). In order to

guarantee that the solution is sufficiently resolved, a number, N_s, of extra (safety) layers of elements may be added to those marked by the gradient criterion at each level.

As discussed elsewhere[19, 20] if explicit temporal descretization schemes are used for this problem the maximum stable time-step is given by $\Delta t \le Ch^2$, where $C = C(\lambda, Le, \Delta T)$, with $C \le 0.001$ found under certain conditions leading to unfeasibly small time-steps. Consequently, an implicit temporal descretization is employed here based on the second order Backward Difference Formula, which is an implicit linear 2-step method, with variable time-step. Rewriting Equations (28) - (30) in operator form

$$\frac{\partial \phi}{\partial t} = F_\phi\left(t,\phi,U,\theta\right),\ \frac{\partial U}{\partial t} = F_U\left(t,U,\phi,\frac{\partial \phi}{\partial t}\right),\ \frac{\partial \theta}{\partial t} = F_\theta\left(t,\theta,\frac{\partial \phi}{\partial t}\right) \tag{38}$$

the second order Backward Difference Formula (BDF2) with variable time-stepping can be written as

$$\frac{1+2r}{1+r}\begin{bmatrix}\phi^{k+1}\\ U^{k+1}\\ \theta^{k+1}\end{bmatrix} - (r+1)\begin{bmatrix}\phi^{k}\\ U^{k}\\ \theta^{k}\end{bmatrix} + \frac{r^2}{1+r}\begin{bmatrix}\phi^{k-1}\\ U^{k-1}\\ \theta^{k-1}\end{bmatrix} = \Delta t\begin{bmatrix}F_\phi\left(t^{k+1},\phi^{k+1},U^{k+1},\theta^{k+1}\right)\\ F_U\left(t^{k+1},U^{k+1},\phi^{k+1},\dot{\phi}^{k+1}\right)\\ F_\theta\left(t^{k+1},\theta^{k+1},\dot{\phi}^{k+1}\right)\end{bmatrix} \tag{39}$$

where, $r = \Delta t_k/\Delta t_{k-1}$ and the choice of time-steps is based on a set of local error estimators in ϕ, U and θ as described in [12]. The method leads to second order convergence in both time and space and the method can be shown to be A-stable[21], so is therefore appropriate for stiff systems of differential equations.

When using implicit time discretisation methods on heavily refined finite difference grids it is necessary to solve a very large, but sparse, system of non-linear algebraic equations at each time-step. Multigrid methods are among the fastest available solvers for such systems and in this work we apply the non-linear generalization known as FAS (full approximation scheme [22]). The local adaptivity is accommodated via the multilevel algorithm originally proposed by Brandt[23]. The interpolation operator is bilinear while injection is used for the restriction

operator. For smoothing the error we use a fully-coupled nonlinear weighted Gauss-Seidel iteration with

$$\phi_{ij}^{k+1} = \phi_{ij}^{k+1} - \omega \frac{\left(F_{\phi}^{*}\left(\phi^{k+1}, U^{k+1}, \theta^{k+1}\right)_{ij} - \left((r+1)\phi_{ij}^{k} - \frac{r^2}{1+r}\phi_{ij}^{k-1} \right) \right)}{\frac{\partial}{\partial \phi_{ij}} F_{\phi}^{*}\left(\phi^{k+1}, U^{k+1}, \theta^{k+1}\right)_{ij}} \tag{40}$$

$$U_{ij}^{k+1} = U_{ij}^{k+1} - \omega \frac{\left(F_{U}^{*}\left(U^{k+1}, \phi^{k+1}, \dot{\phi}^{k+1}\right)_{ij} - \left((r+1)U_{ij}^{k} - \frac{r^2}{1+r}U_{ij}^{k-1} \right) \right)}{\frac{\partial}{\partial U_{ij}} F_{U}^{*}\left(U^{k+1}, \phi^{k+1}, \dot{\phi}^{k+1}\right)_{ij}} \tag{41}$$

$$\theta_{ij}^{k+1} = \theta_{ij}^{k+1} - \omega \frac{\left(F_{\theta}^{*}\left(\theta^{k+1}, \phi^{k+1}, \dot{\phi}^{k+1}\right)_{ij} - \left((r+1)\theta_{ij}^{k} - \frac{r^2}{1+r}\theta_{ij}^{k-1} \right) \right)}{\frac{\partial}{\partial \theta_{ij}} F_{\theta}^{*}\left(\theta^{k+1}, \phi^{k+1}, \dot{\phi}^{k+1}\right)_{ij}} \tag{42}$$

where

$$F_{\phi}^{*}\left(\phi^{k+1}, U^{k+1}, \theta^{k+1}\right) = -\Delta t F_{\phi}\left(t^{k+1}, \phi^{k+1}, U^{k+1}, \theta^{k+1}\right) + \frac{1+2r}{1+r}\phi^{k+1} \tag{43}$$

$$F_{U}^{*}\left(U^{k+1}, \phi^{k+1}, \dot{\phi}^{k+1}\right) = -\Delta t F_{U}\left(t^{k+1}, U^{k+1}, \phi^{k+1}, \dot{\phi}^{k+1}\right) + \frac{1+2r}{1+r}U^{k+1} \tag{44}$$

$$F_{\theta}^{*}\left(\theta^{k+1}, \phi^{k+1}, \dot{\phi}^{k+1}\right) = -\Delta t F_{\theta}\left(t^{k+1}, \theta^{k+1}, \dot{\phi}^{k+1}\right) + \frac{1+2r}{1+r}\theta^{k+1} \tag{45}$$

The number of pre- and post-smoothing operations required for optimal convergence has been investigated within the context of phase-field simulation in [12, 11]. Based on that work we have used V-cycle iteration with 2 pre- and 2 post- smoothing operations at each level.

A major property of the multigrid method is *h*-independent convergence, which means that the convergence rate does not depend on the element size. This behaviour is vital in respect of being able to solve the extreme multi-scale problem arising from coupled thermo-solutal phase-field simulations.

Results

Validation of our numerical scheme against both other coupled phase-field models[10, 7] and, where available, against analytical solutions for pure thermal and pure solutal growth have been reported previously[11, 12, 20], and is therefore not repeated here. The correct

implementation of the anti-trapping current within the model has been validated by reducing the coupled model to the pure solutal case at solutal undercooling Ω by setting $1/Le \to 0$, removing Eq. (30) from the equation set and fixing the system temperature everywhere at $\theta_{sys} = -\Omega$ with $Mc_\infty = 1 - (1-k_E)\,\Omega$ [see 19]. By so doing it is possible to explore the behaviour of the anti-trapping current during the growth of a dendrite under solute only control, wherein we find, in agreement with [9], that solute trapping is suppressed and that the curvature corrected partition coefficient

$$\frac{c_s}{c_l^0} = k[1-(1-k)\frac{d_0}{\rho}] \tag{46}$$

recovers the equilibrium partition coefficient, k_E, to a very high degree of precision. Specifically, for $\Omega = 0.15$ and $k_E = 0.3$ we recover $k = 0.3000 \pm 0.0001$, where this has been tested for λ between 1 and 5 and for h between 0.78 and 0.19 (corresponding to 11 to 13 levels of refinement respectively on a domain of $[-800,800]^2$).

We now consider the partitioning behaviour of the model when we allow a dendrite to grow under coupled thermo-solutal control. Fig. 1 shows the measured (curvature corrected) partition coefficient for a large number of simulations as a function of the dimensionless velocity. All the simulations in this sequence have $k_E = 0.3$, $Mc_\infty = 0.05$, $\lambda = 5$ and $\gamma = 0.02$ and were run with a fixed minimum grid spacing of $h = 0.78$, although the domain size varied between simulations such that interactions between the domain boundary and the thermal field were not encountered. The growth velocity of the dendrite was controlled by varying the undercooling, Δ, in the range 0.1 – 0.8. Lewis numbers in the range 200 - 10000 were considered and are denoted by the symbols in the figure. It is very clear from the figure that despite the presence of an anti-trapping current the measured partition coefficient varies strongly as a function of velocity, with the equilibrium value, k_E, only being recovered as the velocity tends to zero. Moreover, although we have shown elsewhere[20] that the actual growth velocity is a strong function of *Le*, no explicit Lewis number dependence is observed

with all the points corresponding to Lewis numbers in the range 200-10 000 laying, to a very good approximation, on the same curve.

As described above, in experimental solidification studies the observed velocity dependant partition coefficient, $k(V)$, is described by the relationship due to Aziz[13, 14] given in Eq. (1). Should this relationship also hold for the phase-field model, plotting the group $\{(k-k_E)/(1-k)\}$ against V should yield a straight line with gradient $1/V_D = \lambda_i/D_i$. A plot of this type is shown in Fig. 2, where we now also include data for values of the coupling parameters, λ, of 1 and 2 as well as the data shown previously for $\lambda = 5$. As before all simulations are run with $k_E = 0.3$, $Mc_\infty = 0.05$, $\gamma = 0.02$ and with a minimum h of 0.78. The Lewis number in the simulations is, as before, in the range 200 - 10 000, although for clarity we have not indicated the Lewis number in the plot. This is reasonable as we have already demonstrated above that there is no explicit Lewis number dependency. A number of points are apparent from the figure.

Firstly, despite being formulated within the thin interface limit described by [9, 10] the model does have an interface width dependence in so much as solute-trapping is concerned, with a more diffuse interface giving rise to higher levels of solute-trapping. Despite this, in respect of the other main predictive quantities obtained from the model (i.e. V, ρ) the results obtained from the model are indeed independent of the width of the diffuse interface. This has been shown both by Ramirez & Beckermann[7] and ourselves[19, 12], with further evidence being presented in Figure 3, where we show that models with different values of λ, and which therefore display different solute trapping characteristics, give mutually consistent values for V and ρ. Note that here, due to the requirement to keep the group $W_0V/D < 1$[15], the range of accessible values of V decreases as λ increases.

The second point that we note is that the data do, to a reasonable approximation, fit the Aziz model in respect of their velocity dependence. Moreover, if we calculate the slope of the regression line in each of the three cases we obtain, 0.56, 1.09 and 2.75 (for $\lambda = 1$, 2 and 5 respectively), these values displaying an almost exact 1 to 2 to 5 ratio. Equating the gradient

of the regression line with λ_i/D_i and noting that λ_i is the width of the diffuse interface, which within the phase-field model is W_0, itself simply a linear scaling of the coupling parameter λ, we may obtain $D_i = 1.81$. Similar results can be obtained by varying λ over a wider parameter space while keeping all other parameters, including Δ, fixed, an example of which is shown in Fig. 4. Here the model parameters are $k_E = 0.3$, $Mc_\infty = 0.05$, $\gamma = 0.02$, $\Delta = 0.25$, $Le = 200$ and we have plotted the group $\{(k-k_E)/V(1-k)\}$ against λ so that, as above, the gradient may again be directly associated with $1/D_i$. Here we obtain $D_i = 1.91$ by associate λ_i with W_0 (note however that 1/gradient of the line is 1.69 as the graph is plotted against λ, not W_0, to convert to W_0 the scaling factor of a_1 also needs to be applied).

Summary and Conclusions

We have used the phase field model due to Ramirez & Beckermann[7, 10], modified to include an implicit solution capability, to explore how the inclusion of an anti-trapping current within a model of coupled thermo-solutal growth formulated in the thin interface limit actually affects the observed levels of solute trapping during dendritic growth. Contrary to published results for pure solutal models we find that the inclusion of such an anti-trapping current does not lead to the recovery of the equilibrium partition coefficient, except in the limit of very slow growth. At higher growth velocities non-vanishing amounts of solute trapping are observed. Moreover, the extent of this solute trapping is dependant upon the width of the mesoscopic diffuse interface. Indeed, to a good approximation we find that our model recovers the Aziz solute trapping law with a constant interface diffusivity, that is that the solute trapping behaviour may be expressed as a function of the group $\beta = V\lambda_i/D_i$. This result has significant implications for the simulation of the growth of dendrites under coupled thermo-solutal control.

In particular it has hitherto been assumed that provided the phase-field model is constructed within the thin interface formalism, quantitatively valid results may be obtained independent of the width of the diffuse interface, leaving this parameter to be chosen for computational expediency. We now show that this strictly is not the case and that actually λ, and hence W_0, should be chosen so as to match the expected levels of solute trapping. In fact, this is not a

particularly stringent condition as both the results presented here and elsewhere [12, 7, 10] suggest that V, ρ and σ^* do not show a strong dependence on λ, and therefore that they are only weakly effected by solute trapping. This will be particularly true at low undercoolings, where the levels of solute trapping are expected to be low. Conversely, at higher undercoolings and where quantitative predictions of segregation behaviour are required λ may no longer be considered to be a free parameter, wherein it becomes appropriate to enquire as to the appropriate value of λ to yield quantitatively valid solute trapping results.

However, obtaining quantitative evidence for what might constitute an appropriate level of solute trapping is far from straight forward. Experimentally, this is generally presented as a diffusive velocity ($V_D = D_i/\lambda_i$), with estimates varying by up to two orders of magnitude in closely related systems (e.g. from $V_D = 0.37$ m s^{-1} in Si-As [24] to $V_D = 32$ m s^{-1} in Si-Bi [25]). Moreover, there is the possibility that V_D is dependant upon k_E, with values of k_E close to unity giving values of V_D towards the lower end of the spectrum of values. For metal (Al) based systems, which is probably the closest match to the parameter set used here, [26] have reported values for V_D that may be around 5-20 m s^{-1}. Using the results from above we would estimate the equivalent (dimensional) diffusive velocity operating here as $(1.91/W_0)D/d_0$. We have shown previously[20] that the parameter set used here is consistent with Cu- 5wt.% Ni, wherein we obtain $D \approx 3.2 \times 10^{-9}$ m^{2}s^{-1} [27] and $d_0 = 3.7 \times 10^{-10}$ m [28] or $V_D \approx (19/W_0)$ m s^{-1}. This would suggest that W_0 should be adjusted to be between 1-3 to give realistic values of solute trapping.

References

1. A.A. Wheeler, B.T. Murray & R.J. Schaefer, Physica D 1993; 66:243.
2. A.M.Mullis & R.F. Cochrane, Acta Mater. 2001; 49:2205.
3. J.A. Warren & W.J. Boettinger, Acta Metall. Mater. 1995; 43:689.
4. J.R. Green, A.M. Mullis & P.K. Jimack, Metall. Meter. Trans. A 2007; 38:1426.
5. I. Loginova, G. Amberg & J. Aagren, Acta Mater. 2001; 49:573.
6. J.A. Warren & W.J. Boettinger, Acta Metall. Mater. 1995; 43:689.
7. J.C. Ramirez & C. Beckermann, Acta mater. 2005; 53:1721.

8. C.W. Lan, Y.C. Chang, C.J. Shih, Acta mater. 2003; 51:1857.
9. A. Karma, Phys. Rev. E 2001; 87:115701.
10. J.C. Ramirez, C. Beckermann, A. Karma & H.-J. Diepers, Phys. Rev. E 2004; 69:051607.
11. J. Rosam, P.K. Jimack & A.M. Mullis, J. Comp. Phys. 2007; 225:1271.
12. J. Rosam, P. K. Jimack & A. M. Mullis, Acta Mater. 2008; 56:4559.
13. M.J. Aziz, J. Appl. Phys. 1982; 53:1158.
14. M.J. Aziz, Mater. Sci. Eng. A 1994; 178:167.
15. B. Echebarria, R. Folch, A. Karma & M. Plapp, Phys. Rev. E 2004; 70:061604.
16. A.M. Mullis, Comp. Mater. Sci. 2006; 36:345.
17. N. Provatas, N. Goldenfeld & J. Dantzig, J. Comp. Phys. 1999; 148:265.
18. A. Jones & P.K. Jimack, Int. J. Num. Meth. Fluids 2005; 47:1123.
19. J. Rosam, PhD Thesis, University of Leeds, Leeds LS2-9JT.
20. J. Rosam, P. K. Jimack & A. M. Mullis, Phys. Rev. E. 2009; 79:030601.
21. W. Hundsorfer & J.G. Verwer, Numerical Solution of Time-Dependant Advection-Diffusion-Reaction Equations, Springer-Verlag, 2003.
22. U. Trottenberg, C. Oosterlee & A. Schuller, Multigrid, Academic Press (2001).
23. A. Brandt, Math. Comp. 1977; 31:333.
24. J.A. Kittl, P.G. Sanders, M.J. Aziz, D.P. Brunco & M.O Thompson, Acta Mater. 2000; 48:4797.
25. M.J. Aziz, J.Y. Tsao, M.O. Thompson, P.S. Peercy & C.W. White, Phys. Rev. Lett. 1986; 56:2489.
26. P.M. Smith, R. Reitano & M.J. Aziz, Mater. Res. Soc. Symp. Proc. 1993; 279:749.
27. X.J. Han, M. Chen & Y.J. Lu, Int. J. Thermophys. 2008; 29:1408.
28. Smithells Metals Reference Book 7th Edition (Eds. E.A. Brandes & G.B. Brook), Butterworth-Heinemann (1992).

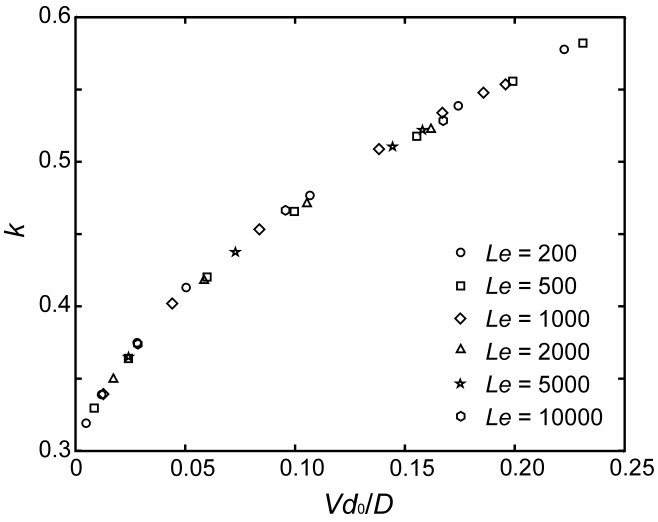

Fig. 1. Measured partition coefficient, k, as a function of growth velocity for the coupled thermo-solutal phase-field model with $k_E = 0.3$, $Mc_\infty = 0.05$, $\lambda = 5$ and $\gamma = 0.02$. Velocity is varied via altering the undercooling Δ.

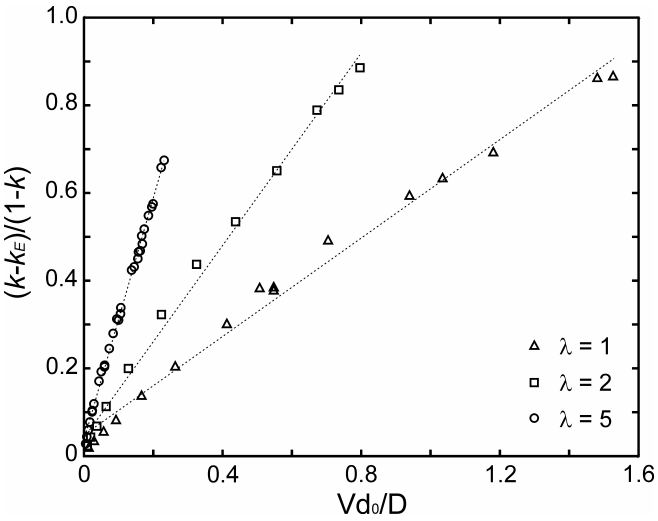

Fig. 2. Solute partitioning behaviour as a function of velocity showing good general agreement with the Aziz model and a dependence upon coupling parameter, λ, (and hence diffuse interface width)

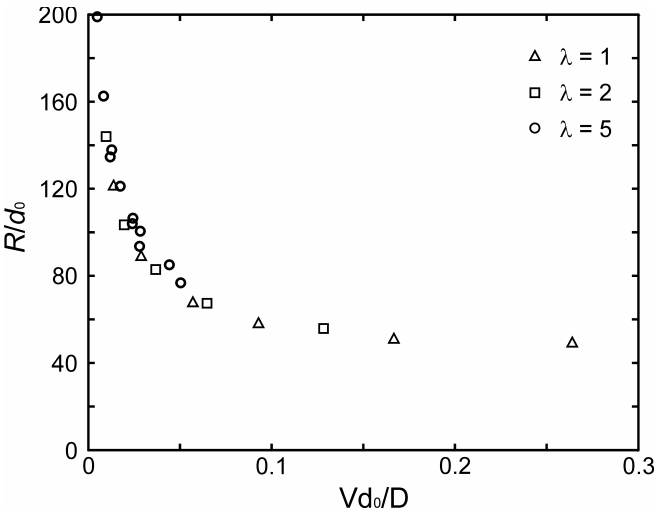

Fig. 3. Dendrite tip radius as a function of velocity for different values of λ, showing that although λ effects the solute trapping characteristics of the dendrite, mutually consistent values for the tip velocity and radius are obtained independent of the value used for λ.

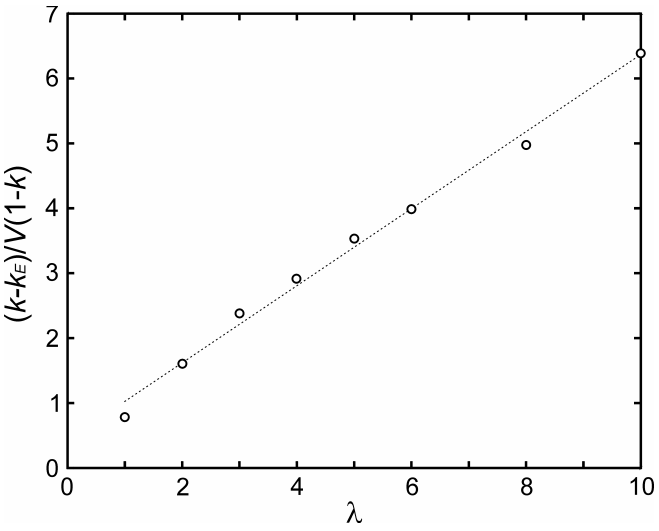

Fig. 4. Solute partitioning behaviour as a function of the coupling parameter, λ, showing good general agreement with the Aziz model.